Entanglement Evolution of Noisy Teleportation

Mohammad Alimoradi Chamgordani[1*] and Henk Koppelaar [2]

[1]Department of Physics, Shahid Chamran University, Ahvaz, Iran

[2]Department of Electronics Engineering, Mathematics and Computer Science, Delft University of Technology, The Netherlands

Abstract: We generalize the teleportation protocol of Bennet et al. to a noisy quantum teleportation protocol (NTP) in which noise factors are corresponded to noisy channels, imperfect measurement and non-maximally entangled channel (isotropic channel). Evolution of entanglement between every two parts of three-partite density matrix changing through five steps of NTP is considered employing concurrence and negativity measures. Then results of concurrence and negativity are evaluated and compared by mutual information as a criterion of correlation. We illustrate the necessity of entanglement in the middle steps of NTP.

Keywords: Quantum information, Entanglement, Noise, Evolution

I. INTRODUCTION

Quantum entanglement is one of the most fascinating topics and also an important source in quantum information applications [1-5]. Quantum teleportation protocol of an unknown d-level system which was described in the original work of Bennet et al. is one of these applications [2]. Teleportation protocol implements classical communication and quantum entanglement to transfer an arbitrary unknown quantum state from a sender (Alice) to a receiver (Bob). In a standard quantum teleportation protocol (STP), an unknown quantum state can be reproduced with complete fidelity F=1, while maximum fidelity using a purely classical channel is F=2/3 [6]. Bennet et al. noted that non-maximally entangled quantum channel reduces the fidelity of teleportation [2]. However not every mixed entangled state can obtain quantum fidelities [7], there are suitable mixed states which do not violate any Bell type inequality but still can be used in teleportation with fidelities greater than the classical bounds [8,9]. Today quantum teleportation has been achieved in laboratories around the world using technology of light polarization [10–16].

Closed quantum systems do not interact with their external environment and they are considered as an ideal model [17]. But in real-world experiments, a quantum system interacts with the environment which is called open quantum system [18]. A pure state in an open quantum system can be changed into a mixed state. Interactions between a system and external environment as dynamical evolution of that system are described by quantum operation. In open quantum systems there are different noises like bit flip, phase flip [19], amplitude damping [17,19] and quantum depolarizing channels [20]. Dynamics of an open quantum system is described by a master equation in the form of Lindblad [21,22]. Fidelity of quantum teleportation subject to various types of noises during different steps of teleportation is achieved by Oh et al. [23] if the noisy quantum channel is described by a single Lindblad operator. Under these conditions, the average fidelity is always greater than 2/3 which is the best obtainable value for classical communication [23]. Iulia et al. studied imperfect one-to-one teleportation and generalized many-to-many teleportation protocol based on non-maximally entangled channel [24]. Badziag et al. [25] showed it is possible to increase the fully entangled fraction [26] (f <1/2) by means of trace preserving LOCC operations and found a class of two-qubit states which can be used for teleportation with non-classical fidelity. Bandyopadhyay [27] analyzed the action of amplitude damping channel for Bell states where the qubits of the entangled pair undergo local interactions with their respective environments. W. Dur et al. [28] obtained fidelity of N pairs (a, c¬1), (c1, c2), … , (cn-1, b), each of the pairs is supposed to be in Werner

state with fidelity F in teleportation of entanglement (entanglement swapping) scheme. Knoll et al. [29] compared degree of agreement between theoretical local environment influences like amplitude damping and dissipative interactions with their experimental results. They investigated influence of particular dissipative interactions by evaluating the quantum fidelity. Local amplitude damping can increase the average teleportation fidelity for a class of entangled states [26,30]. In 2015, all types of noises namely the bit flip, phase flip, depolarizing and amplitude damping channels happening in real world implementations of quantum communication protocols were studied in [31].

Evolution of entanglement through various steps of STP [32]. Also purity and impurity of subsystems of three-partite state across different steps of STP have investigated. In this work we investigate evolution of entanglement on total density matrix describing the initial state through different steps of NTP (generalized case of STP) which ensures the emergence of entangled states in the intermediate steps. Then we compare the results with evolution of entanglement in (STP) [2,32]. To this end, we design NTP scheme and divide it into five steps in which all noise factors involved are noisy channels known as depolarizing channel (an isotropic state) [33], imperfect operations (applied by Bob (BIO)) and finally imperfect measurements on a single qubit by a POVM [34] (performed by Alice (AIM)). After preparing structure of NTP, we analytically obtain mutual information entropy (MIE), conditional entropy (CE) [4], concurrence (C) [35,36] and negativity (N) [37] in each step, and then interpret classical correlation and evolution of entanglement on three-partite state (basically constructed from initial state and isotropic channel) across NTP steps. As we mentioned in the last paragraph fidelity of teleportation subject to various types of noises have investigated in different conditions [23,28-30]. The fidelity of teleportation (in terms of measurements on computational basis) across a Bell channel and also an isotropic channel in which noisy channels (like BIOs) and imperfect measurement (like AIM) involved in, has not achieved yet. Therefore determination of the average fidelities of STP and NTP subjected to denoted noises are other goals will be investigate in this paper. First we obtain average fidelity of STP in the presence of all noises analytically. Then we numerically investigate the BIO effect, the AIM effect and finally both BIO and AIM simultaneously across the Bell channel as the EPR source by plotting different figures. Then we repeat the above procedure for NTP across the isotropic channel a non-maximally mixed state as the EPR source. We show that the two different Bell and isotropic channels give different efficiencies when subjected to the same type of noises.

The other sections of this paper are the following. The physical ideas and mathematical formalism are given in sections II and III. So that an explanation of different noise effects across the quantum teleportation investigated in the following section. In sections IIIA IIIB, correlation and entanglement measures introduced respectively. In section IV quantum circuit of NTP is designed and correlation and entanglement of parts of three-partite density matrix in five steps of NTP are analytically computed and the results are numerically interpreted by plotting curves against noise parameters. Average fidelities of STP (in the presence of noise) and NTP (generalized case) investigated in section V, A and B respectively. Finally section VI is devoted to the description of the results.

II. Modeling Noise: Isotropic Channel, Imperfect Measurement And Operations

Noisy channels are often explained in terms of operator-sum representation as [17,19]:

$$\Theta(\rho) = \sum_{k=1}^{n} A_k \rho A_k^{\dagger}, \tag{1}$$

Where the operation elements A_k, are known as the Kraus operators which for trace preserving operations they satisfy the following condition:

$$\sum_{k=1}^{n} A_k A_k^{\dagger} = I, \tag{2}$$

Where I is the Hilbert space identity. In NTP, the basic idea is that Alice transmits a qubit to Bob through some communications channel with noise or distortion. To this end, depolarizing channel as a simple model for noise in quantum systems is defined according to operator-sum representation as the following [19,20]:

$$\rho_{pure} \xrightarrow{\rho_{ch}^p} \rho_{ch}^p = p\rho_{pure} + \frac{1-p}{d}\mathbf{1}, \qquad (3)$$

d is the dimension for which the condition of complete positivity (CP) is:

$$-\frac{1}{d^2-1} \le p \le 1. \qquad (4)$$

In d dimensions the channel ρ_{ch}^p depends on one real parameter p. This channel maps the pure state ρ_{pure} defined in H^d (Hilbert space) into a linear combination of itself and the $d{\times}d$ identity matrix $\mathbf{1}$. The limit $p \to 0$ corresponds to a very noisy channel, while $p \to 1$ describes a channel with very little noise. The density matrix:

$$\rho_{ch}^{Bell} = \left|\varphi^+\right\rangle\left\langle\varphi^+\right|, \qquad (5)$$

That $\left|\varphi^+\right\rangle = \left(\left|00\right\rangle + \left|11\right\rangle\right)/\sqrt{2}$ as a completely pure Bell state, is mapped to the mixed state:

$$\rho_{ch} = p\left|\varphi^+\right\rangle\left\langle\varphi^+\right| + (1-p)\frac{I}{4}. \qquad (6)$$

In this work we use an isotropic quantum channel as a non-maximally entangled source shared between Alice and Bob in order to be delivered a two-level single qubit in NTP. One reason to use this channel is its convertibility into Bell channel. So by substituting $p = (4F-1)/3$ (in which satisfy Eq. (4)) into Eq. (3), and considering two-qubit form of I from Eq. (2) we obtain:

$$\rho_{isoch}^F = \frac{(4F-1)}{3}\left|\varphi^+\right\rangle\left\langle\varphi^+\right| + \frac{(1-F)}{3}I_{2\times 2}, \qquad (7)$$

Where F and *isoch* denote "isotropic channel" according to F. ρ_{isoch}^F used as EPR source in NTP and is a two-qubit form of [33]:

$$\rho_{iso}^F = \frac{1-F}{d^2-1}\left(\mathbf{1} - \left|\varphi^{AB}\right\rangle\left\langle\varphi^{AB}\right|\right) + F\left|\varphi^{AB}\right\rangle\left\langle\varphi^{AB}\right|, \qquad (8)$$

In which:

$$\left|\varphi^{AB}\right\rangle = \frac{1}{\sqrt{d}}\sum_{i=1}^{d}\left|i^A, i^B\right\rangle, \qquad (9)$$

Is a maximally d dimensional two-partite entangled state and F is defined as following:

$$F := \left\langle\varphi^{AB}\left|\rho_{iso}^F\right|\varphi^{AB}\right\rangle. \qquad (10)$$

As we investigate generalized case of NTP, it is essential to change all perfect measurements and operations used in STP to imperfect measurements and imperfect operations respectively. An imperfect measurement on a single qubit in terms of POVM [28,37] is defined as the following:

$$P_0^\eta = \eta\left|0\right\rangle\left\langle 0\right| + (1-\eta)\left|1\right\rangle\left\langle 1\right|, \qquad (11)$$

$$P_1^\eta = \eta|1\rangle\langle 1| + (1-\eta)|0\rangle\langle 0|, \tag{12}$$

Eqs. (11) and (12) correspond to imperfect projectors. η is accounted as a quantity to determine the situation of the projection onto the basis. Then for $\eta=1$ ideal measurement is obtained. Decreasing η to zero shows entrance of noisy measurement to the system. As a principal system coupled with environment, one can map quantum operation of single qubit and two-qubit gates to general imperfect gate. In open quantum systems some environment distortion effects could be corrected with the operation of bit flip channel (X) and phase flip channel (Z). X and Z are known as Pauli matrices. Thereby in noisy teleportation we need to use imperfect measurements and imperfect form of X, Z and ZX. The action of imperfect operation is represented by two relations [28].

Imperfect one-qubit operation acts on the first qubit (Eq. (13)) and imperfect two-qubit operation acts on qubits 1 and 2 (Eq. (14)) which are defined as the following:

$$O_1\rho = p_1 O_1^{ideal}\rho + \frac{1-p_1}{2} tr_1\{\rho\}\otimes I_1, \tag{13}$$

$$O_{12}\rho = p_2 O_{12}^{ideal}\rho + \frac{1-p_2}{4} tr_{12}\{\rho\}\otimes I_{12}, \tag{14}$$

Where ρ is an entangled state of several qubits, O_1^{ideal} and O_{12}^{ideal} are ideal (perfect) operations act on ρ. In (13) and (14) p_1 and p_2 denote quantities that measure the reliability of operations. $p_j=1$ (j=1, 2) shows ideal operation. Decreasing p_j to zero shows increasing of imperfection in channel and finally increasing noise in system. I_1 and I_{12} express identity operations act on subsystems which O^{ideal} (the perfect operation) acts. We have $p_2 =1$ for an ideal two qubit perfect operation.

III. CORRELATION MEASURES AND ENTANGLEMENT MEASURES

Below we express correlation measures and entanglement measures in subsections A and B respectively.

Mutual Information Entropy (MIE) and Conditional Entropy (CE)
In the fields of quantum statistical and quantum information theory, entropy is accounted as a measure of the disorder and of the missing information about a state. Entropy progressed into a key concept in classical information theory and quantum information theory [1,4,17,19]. Quantum systems used as carriers of information to describe transfer and process of information [4]. The von Neumann entropy of the statistical mixture with the density operator ρ [25,38] is defined by

$$S(\rho) = -\text{Tr}(\rho \log_2 \rho), \tag{15}$$

Where Tr denotes the trace. If the subsystems of a two partite system not to be separable, videlicet they are not independent, therefore the whole system has more information than can be read out of the two subsystems together; so extra information places in correlations between the subsystems. This quantity is named mutual information and we use it as a measure of the degree of correlation of the subsystems [15]. MIE is defined as:

$$\begin{aligned}
S(\rho_a : \rho_b) &= S(\rho_a) + S(\rho_b) - S(\rho_{ab}) \\
&= S(\rho_{ab} \| \rho_a \otimes \rho_b) \geq 0,
\end{aligned} \tag{16}$$

Where $S(\rho_a)$ and $S(\rho_b)$ are the von Neumann entropies of ρ_a and ρ_b, obtained by tracing out system "b" and "a" respectively from ρ_{ab}. $S(\rho_{ab})$ is the von Neumann entropy of the total state. $S(\rho\|\sigma) = \text{Tr}(\rho \log \rho - \rho \log \sigma)$ is quantum

relative entropy. MIE for bipartite quantum systems is non-negative, and bears the interpretation of total correlation between the two subsystems. One can compute conditional entropy (CE) from:

$$S(\rho_a \mid \rho_b) = S(\rho_{ab}) - S(\rho_b)$$
$$= S(\rho_a) - S(\rho_a : \rho_b). \tag{17}$$

Negative values of $S(\rho_a \mid \rho_b)$ can be considered as an effective criterion for measuring of non-separability [19].

Concurrence and Negativity Measures

In order to consider evolution of entanglement through all steps of NTP, we measure entanglement between parts of total density matrix in all steps by concurrence and negativity. Concurrence and negativity as two common powerful measures are used for measuring entanglement of two-qubit systems. Concurrence and negativity measures are introduced as follow respectively:

$$C(\rho_{ab}) = \max_i \left\{ 0, 2\max\left\{\sqrt{\lambda_i}\right\} - \sum_i \sqrt{\lambda_i} \right\}, \tag{18}$$

$$N_d = \left\| \rho_{ab}^{T_a} \right\| - 1, \tag{19}$$

In which Eq. (18) λ_i s are eigenvalues in decreasing order of $R = \rho_{ab}\overline{\rho_{ab}} = \rho_{ab}(Y_a \otimes Y_b)\rho_{ab}^*(Y_a \otimes Y_b)$ where Y_a (Y_b) is the Pauli operator $\begin{pmatrix} 0 & i \\ -i & 0 \end{pmatrix}$. In Eq. (19) $\rho_{ab}^{T_a}$ is the partial transpose with respect to system a, and $\| \ldots \|$ denotes the trace norm. The following section is devoted to analytical computation of correlation in NTP using the mentioned measures.

IV. ANALITICAL COMPUTATION OF CORRELATION IN VARIOUS STEPS OF NTP

In this section, we design an NTP circuit as illustrated in Fig. 1. The top two qubits belong to Alice and the bottom qubit belongs to Bob. We break down NTP in five steps. Our mission is to analytically compute the amount of initially shared entanglement by Alice and Bob among three qubits (a single input qubit ρ_{in} and two qubit channel ρ_{isoch}^F on Fig.1) due to the interaction in five steps of NTP. An unknown quantum state to be teleported can be written as $\left| \psi_{in} \right\rangle = \alpha \left| 0 \right\rangle + \beta \left| 1 \right\rangle$ with $| \alpha |^2 + | \beta |^2 = 1$.

Its density matrix is:

$$\rho_{in} = \left| \psi \right\rangle \left\langle \psi \right| = \begin{pmatrix} |\alpha|^2 & \alpha\beta^* \\ \beta\alpha^* & |\beta|^2 \end{pmatrix}, \tag{20}$$

Where the subscript *in* refers to "input" and $*$ denotes to complex conjugation. It is useful to explain NTP in terms of density operators. To this end we write output state of NTP as the following:

$$\rho_{out} = Tr_{1,2} \left\{ U_{NTP} \rho_{in} \otimes \rho_{isoch}^F U_{NTP}^\dagger \right\}, \tag{21}$$

Where $Tr_{1,2}$ is partial trace over qubits 1 and 2. The unitary operator U_{NTP} is implemented by the teleportation circuit as illustrated in Fig. 1. Actually U_{NTP} is related to noisy channels at steps 2, 5 (ICNOT and BIO respectively), non-maximally entangled isotropic channel and AIMs.

International Journal of Innovative Research in Science, Engineering and Technology
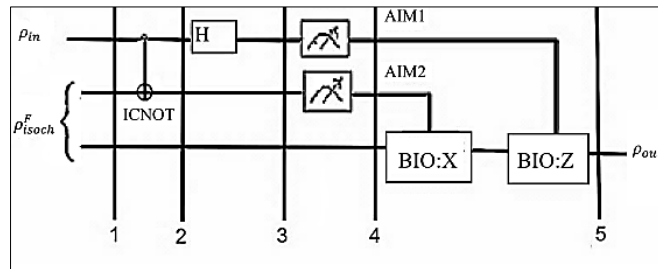
Fig. 1. Quantum circuit in order to teleport the qubit $\left|\psi_{in}\right\rangle$. The two top lines represent Alice's qubits and the bottom line is Bob's qubit. ⟋ means of Alice's imperfect measurements (AIM1 and AIM2). ICNOT, BIO: X and BIO: Z denote noisy channels which the two last correspond to Bob's imperfect operation of X and Z known as Pauli operators. The filled lines mean of delivering classical information (bits).

In STP, the teleported density-matrix, ρ_{out}, is identical to ρ_{in} up to the normalization factor. In subsections that lie ahead, we need to calculate the bounds of entropy, MIE, CE, C and N values finding the extrema affiliated to their analytical functions parameter as:

$$\min\left\{f(\mathbf{x}_i)\right\} \le f(\mathbf{x}_i) \le \max\left\{f(\mathbf{x}_i)\right\}, \tag{22}$$

Where f is one of the mentioned measures in this paper and $\mathbf{x}_i$ are noise parameters involved in each step. These bounds can be used in order to present the properties (purity and impurity) of density matrices. The application of Eq. (22) is presented through Tables 1 to 4 in this paper.

Interaction of Input State ρ_{in} with an Isotropic Channel ρ_{isoch}^{F} at Step 1

The initial total state describing the three qubits before implementing of any quantum operation is given by:

$$\rho_F^{step1} = \rho_{in} \otimes \rho_{isoch}^{F}. \tag{23}$$

The density matrix of Eq. (23) is represented as:

$$\rho_F^{step1} = \begin{pmatrix} A & 0 & 0 & B & C & 0 & 0 & D \\ 0 & E & 0 & 0 & 0 & I & 0 & 0 \\ 0 & 0 & E & 0 & 0 & 0 & I & 0 \\ B & 0 & 0 & A & D & 0 & 0 & C \\ C^* & 0 & 0 & D^* & G & 0 & 0 & H \\ 0 & I^* & 0 & 0 & 0 & J & 0 & 0 \\ 0 & 0 & I^* & 0 & 0 & 0 & J & 0 \\ D^* & 0 & 0 & C^* & H & 0 & 0 & G \end{pmatrix}. \tag{24}$$

In which $*$ denotes to complex conjugation and

$$A = \left(\frac{2F+1}{6}\right)|\alpha|^2, \quad B = \left(\frac{4F-1}{6}\right)|\alpha|^2, \quad C = \left(\frac{2F+1}{6}\right)\alpha\beta^*,$$

$$D = \left(\frac{4F-1}{6}\right)\alpha\beta^*, \quad E = \frac{(1-F)|\alpha|^2}{3}, \quad G = \left(\frac{2F+1}{6}\right)|\beta|^2,$$

$$H = \left(\frac{4F-1}{6}\right)|\beta|^2, \quad I = \frac{(1-F)\alpha\beta^*}{3}, \quad J = \frac{(1-F)|\beta|^2}{3}.$$

The measures MIE, CE, C and N at step 1 between every two parts of ρ_F^{step1} are computed as the following. Conditional entropies (CEs) between each two parts are:

$$S\left(\rho_1^1 \mid \rho_2^1\right) = 0,$$
$$S\left(\rho_1^1 \mid \rho_3^1\right) = 0,$$

$$\tag{25}$$

$$S\left(\rho_2^1 \mid \rho_1^1\right) = 1,$$
$$S\left(\rho_3^1 \mid \rho_1^1\right) = 1,$$

$$\tag{26}$$

$$S\left(\rho_2^1 \mid \rho_3^1\right) = -\log_2\left[2F\left(\frac{3F}{F-1}\right)^{(F-1)}\right],$$

$$\tag{27}$$

Mutual information entropies (MIEs) between each two parts are given by:

$$S(\rho_1^1 : \rho_2^1) = 0,$$
$$S(\rho_1^1 : \rho_3^1) = 0,$$

$$\tag{28}$$

$$S(\rho_2^1 : \rho_3^1) = \log_2\left[4F\left(\frac{3F}{F-1}\right)^{(F-1)}\right],$$

$$\tag{29}$$

Concurrence (C) and negativity (N) between each two parts are:

$$C\left(\rho_{12}^1\right) = 0,$$
$$C\left(\rho_{13}^1\right) = 0,$$

$$\tag{30}$$

$$C\left(\rho_{23}^1\right) = \max[0, 2\max[F, \frac{1-F}{3}] - 1,$$

$$\tag{31}$$

$$N\left(\rho_{12}^1\right) = 0,$$
$$N\left(\rho_{13}^1\right) = 0,$$

$$\tag{32}$$

$$N\left(\rho_{23}^1\right) = \left|\frac{1}{2} - F\right| + F - \frac{1}{2}.$$

$$\tag{33}$$

The superscript 1 is related to the step 1 of NTP. The indices 1, 2 and 3 are related to the first, second and third part of ρ_F^{step1} obtained by tracing out system "23", "13" and "12" from ρ_F^{step1} respectively. The indices 12, 13 and 23 denote to the joint entropies obtained by tracing out system "3", "2" and "1" from ρ_F^{step1} respectively. If one substitutes $F=1$ in ρ_F^{step1}, entropy will be zero that shows a pure density matrix and its density matrix is similar to STP [32]. According to Eq. (22) the bounds of entropy, MIE and CI are determined at step 1 in Table 1. According to Table 1, ρ_{12}^1 and ρ_{13}^1 are always mixed density matrices. For $F=0.24$ the maximally mixed case is obtained for ρ_{23}^1 (ρ_{isoch}^F). $S(\rho_1^1:\rho_2^1)=0$ and $S(\rho_1^1:\rho_3^1)=0$ show inexistence of correlation that is exactly in agreement with related mutual entropy of STP [32]. For $F=1$ (STP) we obtain $S(\rho_2^1:\rho_3^1)=2$ (Fig. 2a). Conditional entropies are $S(\rho_1^1|\rho_2^1)=0$, $S(\rho_1^1|\rho_3^1)=0$ and $-1\leq S(\rho_2^1|\rho_3^1)\leq1$. It means that ρ_{12}^1 and ρ_{13}^1 are separable. Interestingly $S(\rho_2^1|\rho_3^1)$ and $S(\rho_3^1|\rho_2^1)$ are exactly similar and both are negative. For $F=1$, $S(\rho_3^1|\rho_2^1)=-1$ that shows Bell-EPR source as the channel in STP (Fig. 2b). For $F>0.8$ something more than classical correlation (quantum correlation) is shown in Fig. 2: (a) and (b). These results are in accordance with the results of concurrence and negativity at step 1 illustrated in Fig. 2c. For $0\leq F<0.5$ no entanglement is seen. For F greater than 0.5 inseparability is found. In Fig. 2, solid lines and dashed lines illustrate STP and NTP situations respectively.
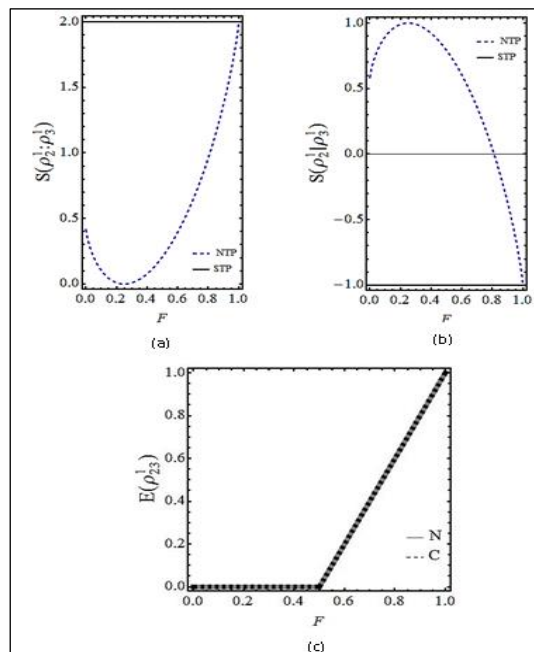
Fig. 2. (a) $S(\rho_2^1:\rho_3^1)$, (b) $S(\rho_2^1|\rho_3^1)$, (c) $E(\rho_{23}^1)$ (concurrence and negativity) as a function of F for α_{max}, β_{max} at step 1.

Effect of ICNOT and the Action of Hadamard (H) Gate on ρ_F^{step1} at Steps 2 and 3

After obtaining ρ_F^{step1} we apply an ICNOT gate achieved from (14) on the first two qubits of ρ_{step1}^F. Then we tend to

$$\rho_{F,p_2}^{step\,2} = p_2\left(CNOT_{12}\otimes I_3\right)\rho_{step1}^F\left(CNOT_{12}\otimes I_3\right)^\dagger + \frac{1-p_2}{4}\left(Tr_{1,2}(\rho_{step1}^F)\otimes I_{12}\right) \tag{34}$$

In which I_3 and I_{12} are 2×2 and 4×4 identity matrices respectively and $CNOT_{12}$ is:

$$CNOT_{12} = \begin{pmatrix} 1 & 0 & 0 & 0 \\ 0 & 1 & 0 & 0 \\ 0 & 0 & 0 & 1 \\ 0 & 0 & 1 & 0 \end{pmatrix} \tag{35}$$

Measures bound		
$S(\rho_1^1) = 0$	$S(\rho_2^1) = 0$	$S(\rho_3^1) = 1$
$S(\rho_{12}^1) = 1$	$S(\rho_{13}^1) = 1$	$0 \le S(\rho_{23}^1) \le 2$
$S(\rho_1^1 : \rho_2^1) = 0$	$S(\rho_1^1 : \rho_3^1) = 0$	$0 \le S(\rho_2^1 : \rho_3^1) \le 2$
$S(\rho_1^1 | \rho_2^1) = 0$	$S(\rho_1^1 | \rho_3^1) = 0$	$-1 \le S(\rho_2^1 | \rho_3^1) \le 2$

Table 1. Entropy, MIE and CE bounds in step 1.

The density matrix of Eq. (34) is represented by:

$$\rho_{F,p_2}^{step\ 2} = \begin{pmatrix}
\frac{(1-p_2)}{8} + Ap_2 & 0 & 0 & 0 & Bp_2 & Dp_2 & Cp_2 & 0 \\
0 & \frac{(1-p_2)}{8} + Ep_2 & 0 & 0 & 0 & 0 & 0 & ip_2 \\
0 & 0 & \frac{(1-p_2)}{8} + Ep_2 & 0 & ip_2 & 0 & 0 & 0 \\
Bp_2 & 0 & 0 & \frac{(1-p_2)}{8} + Ap_2 & 0 & Cp_2 & Dp_2 & 0 \\
0 & 0 & -ip_2 & 0 & \frac{(1-p_2)}{8} + Jp_2 & 0 & 0 & 0 \\
D^*p_2 & 0 & 0 & C^*p_2 & 0 & \frac{(1-p_2)}{8} + Gp_2 & Hp_2 & 0 \\
C^*p_2 & 0 & 0 & D^*p_2 & 0 & Hp_2 & \frac{(1-p_2)}{8} + Gp_2 & 0 \\
0 & -ip_2 & 0 & 0 & 0 & 0 & 0 & \frac{(1-p_2)}{8} + Jp_2
\end{pmatrix}$$

$$\tag{36}$$

In this step the CE, MIE, C and N between each two parts of $\rho_{F,p_2}^{step\ 2}$ are calculated analytically as follows. Conditional entropies (CEs) between each two parts are:

$$S(\rho_1^2 | \rho_2^2) = -\frac{1-p_2}{2} \log_2\left[\frac{1-p_2}{4}\right] - \frac{1+p_2}{2} \log_2\left[\frac{1+p_2}{4}\right] - 1 \tag{37}$$

$$S(\rho_1^2 \mid \rho_3^2) = -T^- \log_2 \left[\frac{T^-}{2} \right] + T^+ \log_2 \left[\frac{T^+}{2} \right] - 1 \tag{38}$$

$$S(\rho_2^2 \mid \rho_3^2) = u \log_2 \left[\frac{u}{2} \right] - S^- \log_2 \left[\frac{S^-}{2} \right] - S^+ \log_2 \left[\frac{S^+}{2} \right] - 1, \tag{39}$$

Mutual information entropy (MIE) between each two parts is:

$$S(\rho_1^2 : \rho_2^2) = 1 - \frac{1 + \Lambda p_2}{2} \log_2 \left[\frac{1 + \Lambda p_2}{2} \right] - \frac{1 - \Lambda p_2}{2} \log_2 \left[\frac{1 - \Lambda p_2}{2} \right] + \frac{1 - p_2}{2} \log_2 \left[\frac{1 - p_2}{4} \right] + \frac{1 + p_2}{2} \log_2 \left[\frac{1 + p_2}{4} \right], \tag{40}$$

$$S(\rho_1^2 : \rho_3^2) = 1 - \frac{1 + \Lambda p_2}{2} \log_2 \left[\frac{1 + \Lambda p_2}{2} \right] - \frac{1 - \Lambda p_2}{2} \log_2 \left[\frac{1 - \Lambda p_2}{2} \right]$$

$$+ u \log_2 \left[\frac{u}{2} \right] + S^- \log_2 \left[\frac{S^-}{2} \right] + S^+ \log_2 \left[\frac{S^+}{2} \right], \tag{41}$$

$$S(\rho_2^2 : \rho_3^2) = 2 + u \log_2 \left[\frac{u}{2} \right] + S^- \log_2 \left[\frac{S^-}{2} \right] + S^+ \log_2 \left[\frac{S^+}{2} \right], \tag{42}$$

in which

$$T^\pm = \frac{1}{2} \pm \frac{p_2}{6} \sqrt{\left(9 + \left(64(F - \frac{1}{4})^2 - 36 \right) |\alpha|^2 |\beta|^2 \right)}, \quad \Lambda = |\alpha|^2 - |\beta|^2, \quad u = -\frac{(4F - 1)p_2 - 3}{6}, \quad S^\pm = \frac{1}{6} \left(3 \pm (4F - 1)\Lambda p_2 \right).$$

Concurrence (C) and negativity (N) between each two parts are given by:

$$C\left(\rho_{12}^2 \right) = 0,$$

$$C\left(\rho_{13}^2 \right) = 0, \tag{43}$$

$$C\left(\rho_{23}^2 \right) = \max \left[0, \frac{1}{2} \max \left[\left| 1 - p_2 + 4p_2 (E + G - H) \right|, \left| 1 - p_2 + 4(E + G + H)p_2 \right|, \right.\right.$$

$$\left| 1 - p_2 + 4(A - B + J)p_2 \right|, \left| 1 - p_2 + 4(A + 4B + 4J)p_2 \right| \right]$$

$$\left. - \frac{1}{4} \left| 1 - p_2 + 4p_2 (E + G - H) \right| - \frac{1}{4} \left| 1 - p_2 + 4p_2 (E + G + H) \right| \right], \tag{44}$$

Measures Bond		
$0 < S(\rho_1^2) \leq 1$	$S(\rho_2^2) = 1$	$S(\rho_3^2) = 1$
$1 \leq S(\rho_{12}^4) \leq 2$	$0 \leq S(\rho_{13}^2) \leq 2$	$0 < S(\rho_{23}^2) < 2$
$0 \leq S(\rho_1^4 : \rho_2^4) \leq 1$	$0 \leq S(\rho_1^2 : \rho_3^2) \leq 1$	$0 \leq S(\rho_2^2 : \rho_3^2) < 2$
$0 \leq S(\rho_1^2 \mid \rho_2^2) \leq 1$	$0 \leq S(\rho_1^2 \mid \rho_3^2) \leq 1$	$-1 \leq S(\rho_2^2 \mid \rho_3^2) < 1$

Table 2. Entropy, MIE, CE bounds in step 2.

$$\text{N}\left(\rho_{12}^2\right) = 0,$$
$$\text{N}\left(\rho_{13}^2\right) = 0, \tag{45}$$

$$\text{N}\left(\rho_{23}^2\right) = \left|\frac{1}{4}+\left(E+G-B-\frac{1}{4}\right)p_2\right| + \left|\frac{1}{4}+\left(B+E+G-\frac{1}{4}\right)p_2\right| + \left|\frac{1}{4}+\left(A-H+J-\frac{1}{4}\right)p_2\right| + \left|\frac{1}{4}+\left(A+H+J-\frac{1}{4}\right)p_2\right| - 1 \tag{46}$$

The bounds of measures in this step using Eq. (22) are shown in Table 2. By the action of ICNOT, pure density matrix ρ_1^1 collapses to mixed density matrix ρ_1^2 and increases impurity of the compound density matrices through step 1 to step 2. Bounds of MIE and CE for ρ_{12}^2 and ρ_{13}^2 show classical correlations between the two parts in this step. Bounds of MIE, CE, C and N for ρ_{23}^2 demonstrate non-separability of the two parts. These results show that the entanglement related to ρ_{23}^2 is not going to be collapsed by the action of ICNOT through step 1 to step 2 but depended on p_2. Figs. 3a-3g show quality of correlations between every two parts of $\rho_{F,p_2}^{step\ 2}$. For ρ_{12}^2, MIE and CE are independent of F but the classical correlation is increased by enhancement of p_2 (Figs. 3a and 3b). For ρ_{13}^2, MIE and CE are depended on both F and p_2 so that by increasing these parameters correlation is raised (Figs. 3c and 3d). For ρ_{23}^2, MIE and CE go beyond the classical limit (1 and 0 respectively) and show entanglement by increasing F or p_2 (Figs. 3e and 3f). In the case of quantum correlation the result of MIE and CE are in accordance with C (Fig. 3g). From Fig. 3 curves, it is found that CE and MIE curves are showing the same concept.
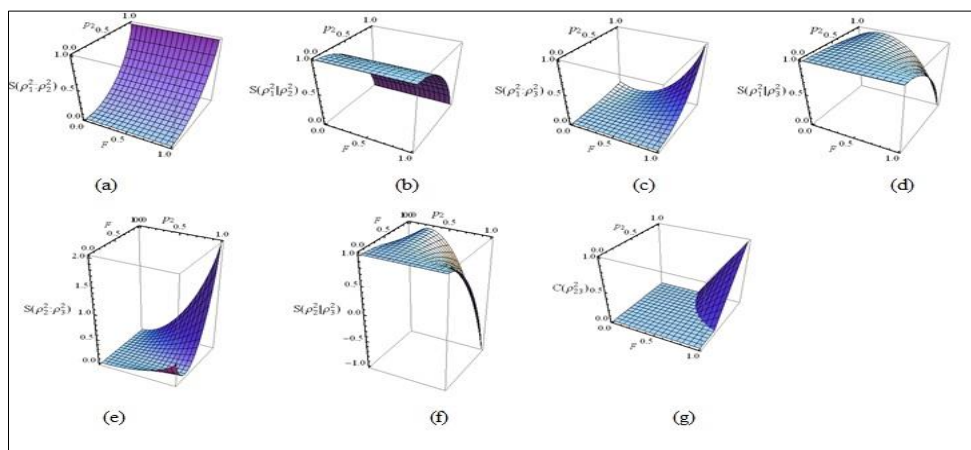
Fig. 3. Representation of classical correlation and entanglement of various partites of $\rho_{F,p_2}^{step\ 2}$ for α_{max}, β_{max}. In (a) $S(\rho_1^2 : \rho_2^2)$ and (b) $S(\rho_1^2 | \rho_2^2)$ show that classical correlation is independent of F and alters by changing p_2. In (c) and (d), $S(\rho_1^2 : \rho_3^2)$ and $S(\rho_1^2 | \rho_3^2)$ show classical correlation alters by changing p_2 and F. In (e) and (f), $S(\rho_2^2 : \rho_3^2)$ and $S(\rho_2^2 | \rho_3^2)$ illustrate entanglement for the values more than 1 and less than 0 respectively. This acclaim is confirmed by the C curve in (g).

Hadamard gate (H) is applied on the first qubit of $\rho_{F,p_2}^{step\,2}$. Then $\rho_{F,p_2}^{step\,2}$ tends to:

$$\rho_{F,p_2}^{step\,3} = \left(\mathbf{H} \otimes I_1 \otimes I_2\right) \rho_{step\,2}^{F,p_2} \left(\mathbf{H} \otimes I_1 \otimes I_2\right)^{\dagger} \qquad (47)$$

In which I_1 and I_2 are 2×2 identity matrices and Hadamard gate is:

$$\mathbf{H} = \frac{1}{\sqrt{2}}\begin{pmatrix} 1 & 1 \\ 1 & -1 \end{pmatrix} \qquad (48)$$

Alice Imperfect Measurements (AIM) at Step 4

STP predicts that once the particles 1 and 2 are projected into one of the four computational bases, particle 3 is instantaneously projected into one of the four pure states found as the matrix coefficients of these bases [32]. In NTP Alice performs imperfect measurements at the computational basis of the joined 12–system of $\rho_{F,p_2}^{step\,3}$. Imperfect two-qubit measurement of Alice in 00 bases has the form of:

$$\begin{aligned} P_{00}^{\eta} = {} & \eta^2 |00\rangle\langle 00| + \eta(1-\eta)|01\rangle\langle 01| \\ & + \eta(1-\eta)|10\rangle\langle 10| + (1-\eta)^2|11\rangle\langle 11|. \end{aligned} \qquad (49)$$

$$\begin{aligned} \rho_{00} = {} & \eta^2 \left(P_{00} \otimes I_3\right) \rho_{step\,3}^{F,p_2} \left(P_{00} \otimes I_3\right)^{\dagger} \\ & + \eta(1-\eta)\left(P_{01} \otimes I_3\right) \rho_{step\,3}^{F,p_2} \left(P_{01} \otimes I_3\right)^{\dagger} \\ & + \eta(1-\eta)\left(P_{10} \otimes I_3\right) \rho_{step\,3}^{F,p_2} \left(P_{10} \otimes I_3\right)^{\dagger} \\ & + (1-\eta)^2 \left(P_{11} \otimes I_3\right) \rho_{step\,3}^{F,p_2} \left(P_{11} \otimes I_3\right)^{\dagger}, \end{aligned} \qquad (50)$$

Imperfect two-qubit measurements of 01, 10, 11 basis could be calculated similarly. If Alice obtains 00 results after measurements, its density operator is expressed as follows in which P_{ij}s are defined as $P_{00} = |00\rangle\langle 00|$, $P_{01} = |01\rangle\langle 01|$, $P_{10} = |10\rangle\langle 10|$, $P_{11} = |11\rangle\langle 11|$. ρ_{10}, ρ_{01} and ρ_{11} can be computed similarly. The general density operator at step 4 is computed as the following:

$$\rho_{F,p_2,\eta}^{step\,4} = \rho_{00} + \rho_{01} + \rho_{10} + \rho_{11} \qquad (51)$$

The density matrix of Eq. (32) is represented as:

$$
\rho_{F,p_2,\eta}^{step\,4} =
\begin{pmatrix}
\frac{S^+}{4} & \frac{D\,p_2}{2} & 0 & 0 & 0 & 0 & 0 & 0 \\
\frac{D^*p_2}{2} & \frac{S^-}{4} & 0 & 0 & 0 & 0 & 0 & 0 \\
0 & 0 & \frac{S^-}{4} & \frac{D^*p_2}{2} & 0 & 0 & 0 & 0 \\
0 & 0 & \frac{D\,p_2}{2} & \frac{S^+}{4} & 0 & 0 & 0 & 0 \\
0 & 0 & 0 & 0 & \frac{S^+}{4} & -\frac{D\,p_2}{2} & 0 & 0 \\
0 & 0 & 0 & 0 & -\frac{D^*p_2}{2} & \frac{S^-}{4} & 0 & 0 \\
0 & 0 & 0 & 0 & 0 & 0 & \frac{S^-}{4} & -\frac{D^*p_2}{2} \\
0 & 0 & 0 & 0 & 0 & 0 & -\frac{D\,p_2}{2} & \frac{S^+}{4}
\end{pmatrix},
\tag{52}
$$

Expression (52) is independent of the parameter η, measure for the quality of the projection onto the basis states. CE for each two parts are computed as follows in step 4:

$$
S(\rho_{1(2)}^4 \mid \rho_{2(1)}^4) = 1,
\tag{53}
$$

$$
S(\rho_{1(3)}^4 \mid \rho_{3(1)}^4) = -\left(\frac{1}{2} + (D+D^*)\,p_2\right)\log_2\left[\frac{0.5+(D+D^*)\,p_2}{2}\right]
$$

$$
-\left(\frac{1}{2} - (D+D^*)\,p_2\right)\log_2\left[\frac{0.5-(D+D^*)\,p_2}{2}\right] - 1
\tag{54}
$$

$$
S(\rho_{2(3)}^4 \mid \rho_{3(2)}^4) = S^+ \log_2\left[\frac{S^+}{2}\right] + S^- \log_2\left[\frac{S^-}{2}\right] - 1
\tag{55}
$$

MIE between each two parts in this step is given by:

$$
S(\rho_1^4 : \rho_2^4) = 0,
\tag{56}
$$

$$
S(\rho_1^4 : \rho_3^4) = 2 + \left(\frac{1}{2} + (D+D^*)\,p_2\right)\log_2\left[\frac{0.5+(D+D^*)\,p_2}{2}\right]
$$

$$
+ \left(\frac{1}{2} - (D+D^*)\,p_2\right)\log_2\left[\frac{0.5-(D+D^*)\,p_2}{2}\right],
\tag{57}
$$

$$
S(\rho_2^4 : \rho_3^4) = 2 + S^+ \log_2\left[\frac{S^+}{2}\right] + S^- \log_2\left[\frac{S^-}{2}\right],
\tag{58}
$$

In which $*$ denotes to complex conjugation. Negativity and Concurrence in this step 4 are computed as the

$$\mathrm{C}\left(\rho_{ij}^4\right) = 0,$$
$$\mathrm{N}\left(\rho_{ij}^4\right) = 0,$$

(59)

Where, $i(=1, 2) < j(= 2, 3)$. According to Eq. (22) the bounds of entropy, MIE and CE, are determined at step 4 in Table 3. From Table 3 some classical correlation between parts one and three as well as two and three is found. There's no negative value for conditional entropy at step 4. At step 4 imperfect measurements are performed by Alice. Moreover, action of measurement not only does not make any entanglement between parts of $\rho_{F,p_2,\eta}^{step\,4}$ through step 3 to step 4, but also makes it separability. The action of noisy measurement diminishes entanglement between parts of general state to zero. In Figs. 4a and 4b show that parts one and three of $\rho_{F,p_2,\eta}^{step\,4}$ are classically correlated as well as parts two and three illustrated in Figs. 4c and 4d.

Measures bound		
$S(\rho_1^4) = 1$	$S(\rho_2^4) = 1$	$S(\rho_3^4) = 1$
$S(\rho_{12}^4) = 2$	$1 < S(\rho_{13}^4) \le 2$	$1 < S(\rho_{23}^4) \le 2$
$S(\rho_1^4 : \rho_2^4) = 0$	$0 < S(\rho_1^4 : \rho_3^4) \le 1$	$0 \le S(\rho_2^4 : \rho_3^4) \le 1$
$S(\rho_1^4 \big| \rho_2^4) = 1$	$0 < S(\rho_1^4 \big| \rho_3^4) \le 1$	$0 \le S(\rho_2^4 \big| \rho_3^4) \le 1$

Table 3. Entropy, MIE, CE bounds.
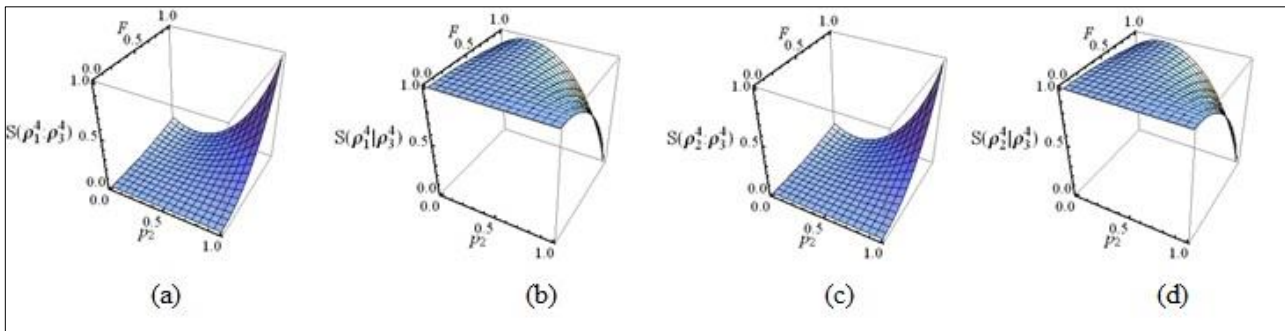
Fig. 4. Scheme of classical correlation of various two parts of $\rho_{F,p_2,\eta}^{step\,4}$ for α_{max}, β_{max}. (a) $S(\rho_1^4 : \rho_3^4)$ and (b) $S(\rho_1^4 | \rho_3^4)$ illustrate classical correlation alters by F and p_2 simultaneously as well as $S(\rho_2^4 : \rho_3^4)$ and $S(\rho_2^4 | \rho_3^4)$ in (c) and (d).

According to Figs. 4a-4d correspond to ρ_{13}^4 and ρ_{23}^4 respectively, by increasing p_2 and F classical correlation is raised and MIE confirms CE.

Bob Imperfect Operation at Step 5

Based on Alice's reports, Bob applies unitary imperfect operators on his qubit. For example if the Alice's measurement result is 00, Bob according to (13) will apply an imperfect unitary matrix on his qubit:

$$\rho_{00}' = \left(I_{12} \otimes I_3^{imper}\right) \rho_{00} = p_1^2 \left(I_{12} \otimes I_3^{per}\right) \rho_{00} \left(I_{12} \otimes I_3^{per}\right)^\dagger$$

$$+\frac{1-p_1}{2}tr_3\left(\rho_{00}\right)\otimes I_3\;.$$

$$\tag{60}$$

ρ'_{01}, ρ'_{10}, and ρ'_{11} are computed similarly and imperfect operators X, Z and ZX are applied on them respectively. Matrix form of the final density operator is:

$$\rho_{F,\eta,p_1,p_2}^{step5}=\begin{pmatrix}\Gamma & \Delta & 0 & 0 & 0 & 0 & 0 & 0\\ \Delta^* & \Omega & 0 & 0 & 0 & 0 & 0 & 0\\ 0 & 0 & \Gamma & \Delta & 0 & 0 & 0 & 0\\ 0 & 0 & \Delta^* & \Omega & 0 & 0 & 0 & 0\\ 0 & 0 & 0 & 0 & \Gamma & \Delta & 0 & 0\\ 0 & 0 & 0 & 0 & \Delta^* & \Omega & 0 & 0\\ 0 & 0 & 0 & 0 & 0 & 0 & \Gamma & \Delta\\ 0 & 0 & 0 & 0 & 0 & 0 & \Delta^* & \Omega\end{pmatrix},$$

$$\tag{61}$$

In which:

Measures bound		
$1\le S(\rho_i^5)\le 1.06$	for	$i\in\{1,2,3\}$
$1.8\le S(\rho_{12}^5)\le 2$	$1\le S(\rho_{13}^5)\le 2$	$1\le S(\rho_{23}^5)\le 2$
$0\le S(\rho_i^5:\rho_j^5)\le 0.31$	for	$i(=1,2)<j(=2,3)$
$0.75\le S(\rho_i^5\vert\rho_j^5)\le 1$	for	$i(=1,2)<j(=2,3)$

Table 4. Entropy, MIE, CE bounds.

$$\Gamma=\frac{1}{8}\left(1-p_1+p_1^2\left(1+p_2\left(\frac{2}{3}[2+F(4\eta-2)-\eta]\Lambda+2|\beta|^2-1\right)\right)\right),\qquad \Omega=\frac{1}{8}\left(1-p_1+p_1^2\left(1+p_2\left(\frac{2}{3}[1-F(4\eta-2)+\eta]\Lambda+2|\beta|^2-1\right)\right)\right),$$

$$\Delta=\frac{p_1^2p_2}{12}\left(4F-1\right)\left(2\eta-1\right)\left(\eta\alpha\beta^*+(1-\eta)\beta\alpha^*\right).$$

CE, MIE, C and N at step 5 are computed as follows:

$$S\left(\rho_i^5\mid\rho_j^5\right)=4\left(\Gamma+\Omega\right),$$

$$\tag{62}$$

$$S\left(\rho_i^5:\rho_j^5\right)=-4\left(\Gamma+\Omega\right)\log_2\left[4\left(\Gamma+\Omega\right)\right],$$

$$\tag{63}$$

$$C\left(\rho_{ij}^5\right)=0,$$

$$N\left(\rho_{ij}^5\right)=0,$$

$$\tag{64}$$

In which $i(=1,2)<j(=2,3)$ and $i\ne j$. At step 5, Bob applies his imperfect operators to reproduce the main state. In this section maximum values of MIE are not large and there's no negative value for CE too. Considering Eq. (22) the

bounds of entropy, MIE and CE are determined at step 5 in Table 4. It is found that there is no eligible correlation between any two parts of $\rho_{F,\eta,p_1,p_2}^{step5}$ from Table 4.

V. CONCLUSION

In summary, we designed an NTP in which most possible noise factors in various steps have been added. All these noise factors appeared in the highest or lowest values in teleportation process. We analyzed the purity and derived the behavior of the entanglement in different steps of NTP. Looking at Tables 1-4 the initial pure ρ_1^k (k=1..5, is devoted to the number of steps) in step one evolves to a mixed state in step 5. ρ_2^k and ρ_3^k stay mixed through all steps. Entropy of ρ_{ij}^k in which $i(=1,2) < j(=2,3)$ (i, j denote partite indices) increases through step 1 to step 5. So the purity of ρ_{ij}^k is decreased. According to Table 1, there is no entanglement between parts one and two nor is it between one and three at step 1. However between parts two and three there's correlation that depends on the fidelity of F which has been revealed in isotropic channel. Then for $0 \le F \le 1/2$ the entanglement of common pair is zero. Applying an ICNOT gate on the first two parts of ρ_{step1}^F tend to create correlation between part one and two as well as one and three. Applying Hadamard gate doesn't change the conditions therefore the emergence of the entangled states in the intermediate steps is ensured. The MIE $S(\rho_1^2:\rho_3^2)$ becomes non-zero before performing quantum measurement which seems to be consistent with original purpose of the quantum teleportation. By implementing an imperfect measurement at step 4, the entanglement between any two parts would vanish. Our computations show there's no entanglement between any two parts of $\rho_{F,\eta,p_1,p_2}^{step5}$.

REFERENCES

[1] J. Audretsch, Entangled world: the fascination of quantum information and computation, ILLY-VCH. Tandem Verlag GmbH, Germany, 2006.
[2] C. H. Bennett, G. Brassard, C. Crepeau, R. Jozsa, A. Peres and W. K. Wootters, Phys. Rev. Lett. 70, 13, 1993.
[3] A. K. Ekert, Phys. Rev. Lett. 67, 6, 1991.
[4] J. Audretsch, Entangled systems: new directions in quantum physics, ILLY-VCH. Tandem Verlag GmbH, Germany, 2007.
[5] G. Jaeger, Quantum information,Springer, New York 2007.
[6] S. Massar and S. Popescu, Phys. Rev. Lett. 74, 8, 1995.
[7] C. H. Bennett, G. Brassard, S. Popescu, B. Schumacher, J. A. Smolin and W. K. Wootters, Phys. Rev. Lett. 76, 5, 1996.
[8] R. Horodecki, M. Horodecki and P. Horodecki, Phys. Rev. A 60, 3, 1999.
[9] S. Popescu, Phys. Rev. Lett. 72, 6, 1994.
[10] D. Bouwmeester, J. W. Pan, K. Mattle, M. Eibl, H. Weinfurter and A. Zeilinger, Nature 390, 6660 ,1997.
[11] R. Ursin, T. Jennewein, M. Aspelmeyer, R. Kaltenbaek, M. Lindenthal, P. Walther and A. Zeilinger, Nature 430, 7002 ,2004.
[12] D. Boschi, S. Branca, F. De Martini, L. Hardy and S. Popescu, Phys. Rev. Lett. 80, 6 , 1998.
[13] X.-M. Jin, J. G. Ren, B. Yang, Z. H. Yi, F. Zhou, X.F. Xu, S. K. Wang, D. Yang, Y. F. Hu, S. Jiang, T. Yang, Nature Photonics 4, 6 ,2010.
[14] Y.-H. Kim, S. P. Kulik & Y. Shih, Phys. Rev. Lett. 86, 7, 2001.
[15] Yin., F. Yue, D. F. McCleary, Z. Ye, L. Edsall, S. Kuan, U. Wagner, J. Dixon, L. Lee, V. V. Lobanenkov and B. Ren, Nature 488, 7409 ,2012.
[16] X-S. Ma, T. Herbst, T. Scheidl, D. Wang, S. Kropatschek, W. Naylor, B. Wittmann, A. Mech, J. Kofler, E. Anisimova and V. Makarov, Nature 489, 7415 ,2012.
[17] D. McMahon, Quantum computing explained,Wiley, New Jersey, 2007.
[18] H. Breuer and F. Petruccione, The theory of open quantum systems,Oxford University Press on Demand, New York, 2002.
[19] M. A. Nielsen and I. L. Chuang, Quantum computation and quantum information, Cambridge University Press, Cambridge, 2000.
[20] C. King, IEEE Trans. Inf. Theory 49, 1, 2003.
[21] G. Lindblad, Commun. Math. Phys. 48, 2, 1976.
[22] R. Alicki and K. Lendi, Quantum Dynamical Semigroups and Applications, Lecture Notes in Physics, Springer-Verlag, Berlin, 1987.
[23] S. Oh, S. Lee, and H. Lee, Phys. Rev. A 66, 022316, 2002.
[24] I. Ghiu, Rom. J. Phys 57, 077125, 2012.
[25] C. H. Bennett, D. P. DiVincenzo, J. A. Smolin and W. K. Wootters, Phys. Rev. A 54, 3824 ,1996.
[26] P. Badziag, M. Horodecki, P. Horodecki, and R. Horodecki, Phys. Rev. A 62, 012311, 2000.
[27] S. Bandyopadhyay, Phys. Rev. A 65, 022302, 2002.
[28] W. Dur, H. J. Briegel, J. I. Cirac and P. Zoller., Phys. Rev. A 59, 169 ,1999.
[29] L. T. Knoll, C. T. Schmiegelow, and M. A. Larotonda, Phys. Rev. A 90, 042332, 2014.

[30]   Y. Yeo, Phys. Rev. A 78, 022334, 2008.
[31]   R. Fortes and G. Rigolin, Phy. Rev. A 92, 012338, 2015.
[32]   Y. H. Ju, E. Jung, M. Hwang, D. K. Park, H. Kim, M. Kim, J. Son, S. Yoo, S. Tamaryan, arXiv:0707.1227.
[33]   S. Lee, D. P. Chi, S. D. Oh and J. Kim, Phys. Rev. A 68, 062304, 2003.
[34]   C. W. Helstrom, J. Stat. Phys. 1, 231, 1969.
[35]   S. Hill and W. K. Wootters, Phys. Rev. Lett. 78, 5022, 1997.
[36]   W. K. Wootters, Phys. Rev. Lett. 80, 2245, 1998.
[37]   G. Vidal, and R. F. Werner, Phys. Rev. A 65, 32314, 2002.
[38]   C. Bennett, H. Bernstein, S. Popescu and B. Schumacher, Phys. Rev. A 53, 4 ,1996.